Journal of Physics:
Conference Series

PAPER • **OPEN ACCESS**

An Effective Small Electrodynamic Shaker Modeling Method

To cite this article: Jinpeng Li *et al* 2023 *J. Phys.: Conf. Ser.* **2457** 012026

An Effective Small Electrodynamic Shaker Modeling Method

Jinpeng Li[1], Ke Deng[1], Gang Wang[1, *], Gangming Zhang[2], Zhiqing Bai[2], Lu Yang[2]

[1]Aerospace Science & Industry Corp Defense Technology R&T Center, Beijing 100854, China

[2]College of Electrical Engineering and Control Science, Nanjing Tech University, Nanjing 211899, China

[*]w_gang99@sina.com

Abstract. Currently, the discussion on the modeling method characterized by the small electrodynamic shakers, especially the mathematic analytical method, is relatively sparse. In this paper, taking BK4809 as an example, a modeling method for small shakers based on analytical formulations is discussed. The detailed mathematical analysis and derivation process for the small shakers are performed, and the corresponding modeling formulations are concluded; then, the simulation tests are carried out in MATLAB. Through comparison with the reference data, the validation tests show that based on analytic formulations combined with the MATLAB built-in system identification functions, the results of modeling methods match well with the experiment data, and the concluded method is effective.

1. Introduction

As to the vibration tests, the virtual shaker test (VST) is a novel approach for improving vibration test performance introduced in 2007. By performing VST, researchers could evaluate the performance of the shaker and the tested object and avoid overtesting them. Refs. [1,2] introduce the fundamentals and physics of the electrodynamic shaker performance. Ref. [3] presents the virtual simulation tool for the ESA QUAD Head Expander, which is a 3m*3m large electrodynamic shaker. The implications indicate that VST could provide reliable test performance and improve the model correlation. Ref. [4] describes the VST procedure with the use of the practical application of the spacecraft BepiColombo on the large shaker QUAD. Ref. [5] presents a similar research case. Ref. [6] demonstrates the progress of a TAS activity in exploring the VST approach, which employs another large shaker Atlas located in the facility of TAS-Cannes and a spacecraft. Ref. [7] adopts a similar large shaker to perform the satellite vibration test, then, based on the experiment data, combined with CARMA model identification methods to estimate the related parameters.

The modeling of the shaker is the basis of the VST, and the main focuses of the above research are on the VST application for huge spacecraft based on the large electrodynamic shaker. However, a detailed discussion about the modeling methods, especially for the small shakers, has been rarely explored, with only several papers underlined. Specifically, we can apply analytical formulations and modal analysis to estimate parameters to model the shaker. Ref. [8] adopts analytical formulations to model a small shaker. The parameters calculation formulations are given, but the detailed mathematical analysis and derivation process is not provided. Ref. [9] mainly introduces the modeling methods for a small shaker based on modal analysis; the discussion about analytical formulations is also inadequate.

This paper discusses a modeling method for small shakers based on analytical formulations. We execute a detailed systematic analysis to access the mathematic expressions for the small shakers in Section 2. Further, based on the derived analytic formulations, combined with MATLAB to estimate shaker modeling parameters in Section 3. Section 4 performs comparisons between the simulation data and the experiment data to validate the modeling method and contains conclusions.

2. Lumped parameter electrodynamic shaker model

Electrodynamic shakers have the advantages of being relatively inexpensive, simple to control, and have approximately linear behavior, and are widely used in vibration tests. As shown in Figure 1(a), the core of the shaker is the coil, which is wound around a stiff thin-walled tube and forms the coil form. The coil form is suspended in a magnetic field between the inner pole and the outer pole, one end of the coil form is attached directly to the vibration table, and the other end of that is attached to a compliant disk. We often call the coil (coil form) and the table combination as armature ($M_{armature}$). The shaker adopts these flexure supports to keep the coil form concentric between poles and restrain any out-of-plane moments applied to the vibration table. When the current flows through the coil, a force F_{coil} is produced in proportion to the current i and is transmitted to the test object, which is affixed to the vibration table. By reaction, the force F_{coil} is also operated on to the shaker body. Meanwhile, as the coil moves axially in the magnetic field, a back-emf $U_{backemf}$ is generated in proportion to the velocity across the coil and reflects the mechanical activity into the electrical domain, which means a "two-way street" between the mechanical and electrical parts and these two are coupled. The power amplifier has two operation modes: voltage and current. In the former mode, E is related to the input voltage V, in which the current i flowing into the coil depends on the mechanical movements. This leads to evident electromagnetic damping when the movement of the armature exhibits a maximum around the resonance frequency. In the latter mode, the output of the amplifier is the current i. For the current independent of the $U_{backemf}$, the mechanical movement of the shaker affects V, which means that there is no electromagnetic damping effect. The vibration shaker applications typically adopt the voltage amplifier.

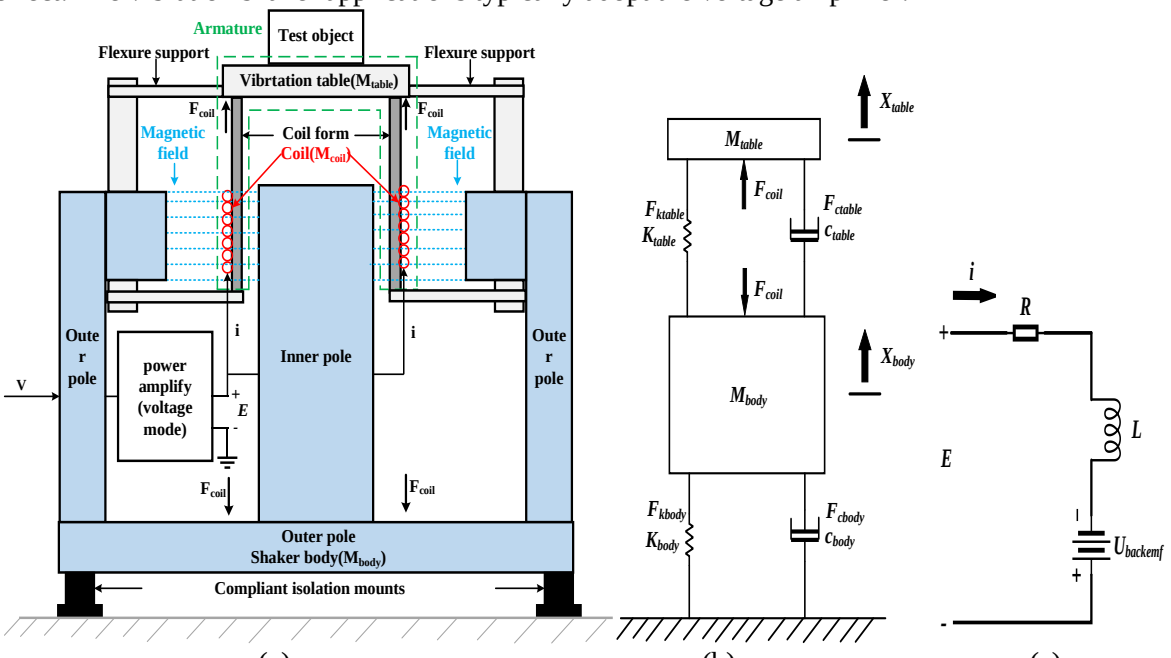

Figure 1. (a)The structure of the electrodynamic shaker; (b)The modeling of the mechanical part of the small shaker; (c)The modeling of the electrical part of the small shaker.

As shown in Figure 1(b), for the small shaker, the vibration table and the coil are considered as one rigid body, and the coil mass is ignored. Through an elastic suspension system adopting a pierced

compliant disk that provides radially distributed cantilevers between the shaker body and vibration table, the table is allowed to move axially. We recognize this compliant connection as a 1 DOF spring and damping system. The shaker body uses the compliant mounts to gain isolation from the floor, which is also modeled by adopting 1 DOF spring+damping to attach the shaker body and the floor. Therefore, the mechanical part is a 2 DOFs system. Figure 1(c) depicts the electrical part, and we should account for the resistance *R*, and the inductance *L* of the coil, and μ_{emf} is the back-emf coefficient of the shaker. The mechanical part is ignited by force F_{coil} proportional to the current *i* of the electrical part. Meanwhile, the electrical part is excited by the back-emf $U_{backemf}$ proportional to the coil velocity of the mechanical part. Therefore, these two parts are cross-coupled, and the small shaker is a 3 DOFs coupled system. The M_{table}, K_{table}, and C_{table} are the mass, stiffness, and damping of the vibration table. The M_{body}, K_{body}, and C_{body} are the mass, stiffness, and damping of the shaker body. X_{table}, X_{body}, F_{ktable}, F_{kbody}, F_{ctable}, and F_{cbody} are the related displacement, stiffness force, and damping force of the table and body, respectively.

For the mechanical part of the small shaker, the upward motion is assumed as positive. The vibration table moves upward and X_{table} is greater than X_{body}. As shown in Figure 2(a), we have the following equations:

$$F_{coil} - F_{ktable} - F_{ctable} = M_{table}\ddot{X}_{table} \tag{1}$$

$$F_{ktable} = K_{table}(X_{table} - X_{body}) \tag{2}$$

$$F_{ctable} = C_{table}(\dot{X}_{table} - \dot{X}_{body}) \tag{3}$$

$$F_{coil} = \mu_{force} i \tag{4}$$

Equations (2) to (4) are substituted into Equation (1), and the following Equation (5) is obtained:

$$M_{table}\ddot{X}_{table} + C_{table}\dot{X}_{table} - C_{table}\dot{X}_{body} + K_{table}X_{table} - K_{table}X_{body} - \mu_{force} i = 0 \tag{5}$$

As to the vibration table, we assume the shaker body moves upward, X_{body} is greater than X_{table}. As shown in Figure 2(b), the following equations are obtained:

$$-F_{kbody} - F_{ktable} - F_{coil} - F_{ctable} - F_{cbody} = M_{body}\ddot{X}_{body} \tag{6}$$

$$F_{ktable} = K_{table}(X_{body} - X_{table}) \tag{7}$$

$$F_{ctable} = C_{table}(\dot{X}_{body} - \dot{X}_{table}) \tag{8}$$

$$F_{kbody} = K_{body}X_{body} \tag{9}$$

$$F_{cbody} = C_{body}\dot{X}_{body} \tag{10}$$

Equations (7) to (10) and Equation (4) are substituted into Equation (6), and the following Equation (11) is obtained:

$$M_{body}\ddot{X}_{body} + (C_{table} + C_{body})\dot{X}_{body} - C_{table}\dot{X}_{table} + (K_{body} + K_{table})X_{table} - K_{table}X_{table} + \mu_{force} i = 0 \tag{11}$$

As shown in Figure 2(b), according to the RL circuit, we have the following Equations:

$$E = Ri + L\frac{di}{dt} + U_{backemf} \tag{12}$$

$$U_{backemf} = \mu_{emf}(\dot{X}_{table} - \dot{X}_{body}) \tag{13}$$

Equation (13) is substituted into Equation (11), and the following Equation (13) is obtained:

$$\mu_{emf}\dot{X}_{table} - \mu_{emf}\dot{X}_{body} + L\frac{di}{dt} + Ri = E \tag{14}$$

We set state vector $\{\boldsymbol{X}\} = \{X_{table}\ X_{body}\ i\}^{\mathrm{T}}$, then rearrange Equations (5), (11), and (14), and the small shaker system expression could be described as follows:

$$\begin{pmatrix} M_{table} & 0 & 0 \\ 0 & M_{body} & 0 \\ 0 & 0 & 0 \end{pmatrix}\begin{pmatrix} \ddot{X}_{table} \\ \ddot{X}_{body} \\ 0 \end{pmatrix} + \begin{pmatrix} C_{table} & -C_{table} & 0 \\ -C_{table} & C_{table}+C_{table} & 0 \\ \mu_{emf} & -\mu_{emf} & L \end{pmatrix}\begin{pmatrix} \dot{X}_{table} \\ \dot{X}_{body} \\ \frac{di}{dt} \end{pmatrix} + \begin{pmatrix} K_{table} & -K_{table} & -\mu_{force} \\ -K_{table} & K_{body}+K_{table} & \mu_{force} \\ 0 & 0 & R \end{pmatrix}\begin{pmatrix} X_{table} \\ X_{body} \\ i \end{pmatrix} = \begin{pmatrix} 0 \\ 0 \\ E \end{pmatrix} \tag{15}$$

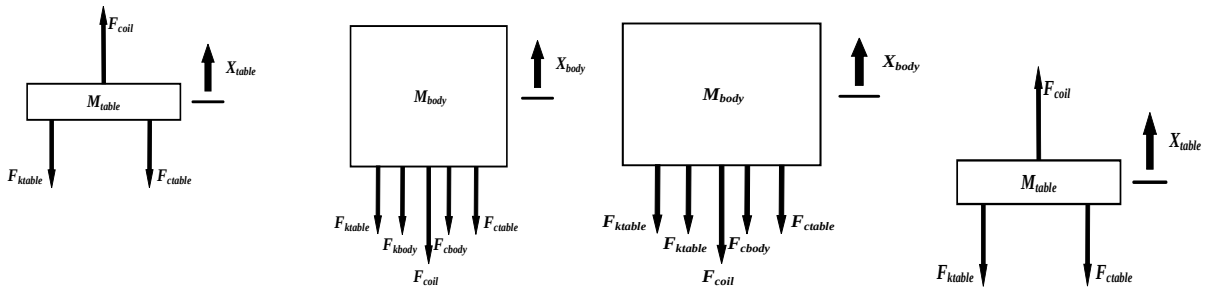

(a) (b) (c) (d)

Figure 2. (a)The free-body diagram of the table of the small shaker; (b) The free-body diagram of the body of the small shaker; (c) The free-body diagram of the free body;(d) The free-body diagram of the free table.

3. Parameter determination

To achieve the virtual shaker modeling, we need to determine the values of the mechanical and electrical parameters demonstrated in Equation (15). We take the 3 DOFs small shaker BK4809 as examples to describe the methods to achieve parameter determination. BK4809 has a diameter of about 0.15m and a height of about 0.14m. It can impart the force rating to a 45N sine peak, and the frequency range is from 10 Hz to 20 kHz. The data acquisition system is formed by using LMS SCADAS III, FLUKE AC probes, and impedance heads. The displacement and acceleration data are measured through the sensors on the related objects.

For the small shaker, we could alternatively block each DOF and confirm only one DOF moves to estimate parameters [9]. As to the BK4809, we make two configurations: the shaker with a free table (the shaker without isolation studs) and the shake with a free body (mounting a rigid structure block the table), and the electrical DOF is also eliminated by shortening the coil. Firstly, we block the table and only let the body oscillates, as shown in Figure 2(c), the body is assumed to move upward and X_{table} is zero. The force equations are as follows:

$$-F_{kbody} - F_{ktable} - F_{ctable} - F_{cbody} - F_{coil} = M_{body}\ddot{X}_{body} \tag{16}$$

$$F_{coil} = \mu_{force} i \tag{17}$$

$$F_{kbody} = K_{body} X_{body} \tag{18}$$

$$F_{ktable} = K_{table} X_{body} \tag{19}$$

$$F_{cbody} = C_{body}\dot{X}_{body} \tag{20}$$

$$F_{ctable} = C_{table}\dot{X}_{body} \tag{21}$$

According to Equations (16) to (21), we get the Laplace transformation expression of the transfer function for the shaker body:

$$\frac{X_{body}(s)}{i(s)} = \frac{-\mu_{force}}{M_{body}s^2+(C_{body}+C_{table})s+(K_{body}+K_{table})} = \frac{-\mu_{force}}{M_{body}} \frac{1}{s^2+\frac{C_{body}+C_{table}}{M_{body}}s+\frac{K_{body}+K_{table}}{M_{body}}} \quad (22)$$

Secondly, we fix the body and only let the table free, as shown in Figure 2(d), the table is assumed to move upward and X_{body} is zero. The force equations are as follows:

$$F_{coil} - F_{ktable} - F_{ctable} = M_{table}\ddot{X_{table}} \quad (23)$$

$$F_{ktable} = K_{table}X_{table} \quad (24)$$

$$F_{ctable} = C_{table}\dot{X_{table}} \quad (25)$$

According to Equations (17), (23) to (25), we get the Laplace transformation expression of the transfer function for the shaker table:

$$\frac{X_{table}(s)}{i(s)} = \frac{\mu_{force}}{M_{table}s^2+(C_{table})s+(K_{table})} = \frac{\mu_{force}}{M_{table}} \frac{1}{s^2+\frac{C_{table}}{M_{table}}s+\frac{K_{table}}{M_{table}}} \quad (26)$$

Then for each DOF, we conduct two different experiments to collect the input and output data to estimate the corresponding transfer functions. The two input signals are sine wave and pulse wave, representing the coil current i, and the frequencies are 10 Hz and 0.5 Hz. For the free body DOF, the estimated transfer function of Equation (22) is $\frac{-1.889}{s^2+51.04s+3.047e04}$, the MSE and the FPE of which are 9.062e-18 and 1.1e-11, and the fits between the two experimental data and the estimated output are 96% and 83%. The estimated transfer function of Equation (26) is $\frac{101.9}{s^2+206s+1.597e05}$, the MSE and the FPE of which are 1.001e-10 and 1.001e-10, and the fits between the two experimental data and the estimated output are 97% and 95%.

At last, based on the above descriptions, we arrange the following Equations (27) and (28) to calculate the mechanical parameters, where $\frac{\mu_{force}}{M_{body}} = 1.889, \frac{C_{body}+C_{table}}{M_{body}} = 51.04, \frac{K_{body}+K_{table}}{M_{body}} = 3.047e04, \frac{\mu_{force}}{M_{table}} = 101.9, \frac{C_{table}}{M_{table}} = 206, \frac{K_{table}}{M_{table}} = 1.597e05$. The manufacturer gives the value of M_{table} is 0.06kg. Therefore, the other values of parameters are $\mu_{force} = 6.114\text{N/A}, C_{table} = 12.36\text{N/(m/s)}, C_{body} = 153.0096\text{N/(m/s)}, K_{table} = 0.09582e05\text{N/m}, K_{body} = 8.91408e04\text{N/m}, M_{body} = 3.24\text{kg}$.

$$\frac{-\mu_{force}}{M_{body}} \frac{1}{s^2+\frac{C_{body}+C_{table}}{M_{body}}s+\frac{K_{body}+K_{table}}{M_{body}}} = \frac{-1.889}{s^2+51.04s+3.047e04} \quad (27)$$

$$\frac{\mu_{force}}{M_{table}} \frac{1}{s^2+\frac{C_{table}}{M_{table}}s+\frac{K_{table}}{M_{table}}} = \frac{101.9}{s^2+206s+1.597e05} \quad (28)$$

Then we should identify the electrical parameters. *R* and *L* are obtained by a simple measurement on the RLC meter, and the values are 1.34Ω and 74.8 μH. The electrical DOF has the following Equation:

$$Ri + L\frac{di}{dt} + \mu_{emf}\left(\dot{X_{coil}} - \dot{X_{body}}\right) = E \quad (29)$$

We assume $i = Ie^{j\omega t}$, $X_{coil} = X_c e^{j\omega t}$, $\dot{X_{coil}} = j\omega X_c e^{j\omega t} = j\omega X_{coil}$, $X_{body} = X_b e^{j\omega t}$ and $\dot{X_{body}} = j\omega X_b e^{j\omega t} = j\omega X_{body}$, then the above Equation could be changed as the following in the frequency domain.

$$(R + j\omega L)i + j\omega\mu_{emf}\left(X_{coil} - X_{body}\right) = E \quad (30)$$

As described before, we could assume the movement of the coil (X_{coil}) is equal to that of the table in the suspension mode, which is much higher than X_{body}. Therefore, this eventually leads to:

$$(R + j\omega L)i + j\omega\mu_{emf}X_{coil} = E \quad (31)$$

For calculation convenience, we rearrange it as:

$$R + j\omega L + \frac{\mu_{emf}}{j\omega}\frac{\ddot{X_{coil}}}{i} = \frac{E}{i} \tag{32}$$

From measurements, the coil acceleration and the related FRFs are available in the suspension mode. Then over the considered frequency, the equation for each spectral line is achieved and μ_{emf} is calculated by solving the resulting least-squares problem in MATLAB, the value of which is about 6.096V/(m/s).

4. The validation test and conclusions

Based on the values determined in Section 3, we can now perform simulation tests through MATLAB based on the state-space models derived from the modeling expressions of Equation (15), the results of which are then compared with the experimental data to validate the modeling methods. The input signal is a 10s sweep sine wave, and the frequency range is from 1 Hz to 1000 Hz. For the small shaker BK4809, the time domain response displacement comparison of the shaker's table is provided in Figure 3. Also, the noise is included in the experiment data and not in the simulation data. The predicted level is obedient to the experiment level. Figures 4 and 5 depict the stabilization diagrams and the amplitude spectrum of the shaker's table in the frequency domain, where the solid red line and the dotted green line represent the experiment and the simulation, respectively. Though there exist some differences, these curves clearly show the natural frequencies of the shaker, and the results match well with the experiment data. Therefore, the modeling method for the small type of shakers based on the analytic mathematic formulations is effective.

This paper proposes an effective modeling method for small electrodynamic shakers. Sections 2 and 3 describe the analytic mathematic formulation modeling method in detail, and the validation is proved through validation tests. Through systematic analysis, several conclusions can be drawn as follows: the established shaker models have been implemented in the linear state-space simulation environment for which the executed sine sweeps demonstrate the correlation with the experimentally observed behavior. It should be noted that the modeling methods are based on the assumption that some shakers' parameters as constant and that they are not, and this is a factor leading to the simulation error.

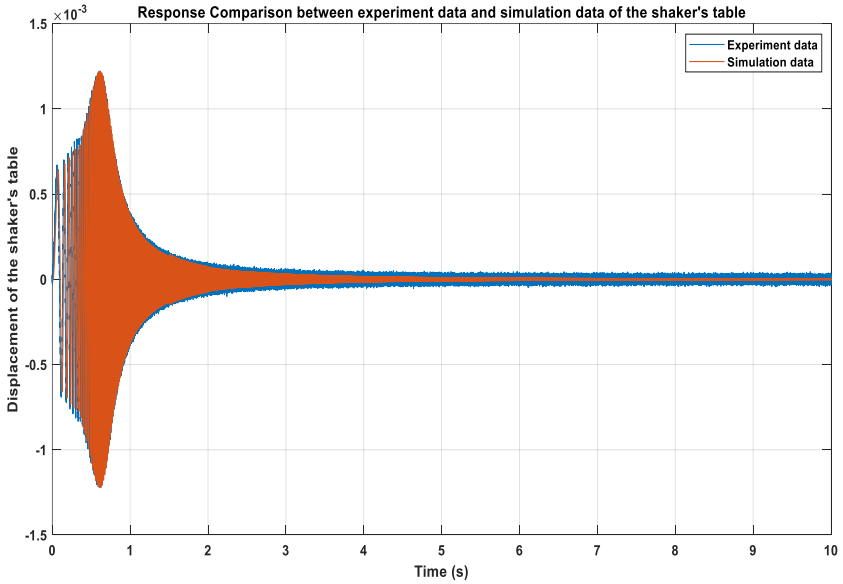

Figure 3. Comparison between experiment and simulation of the displacement of shaker's table.

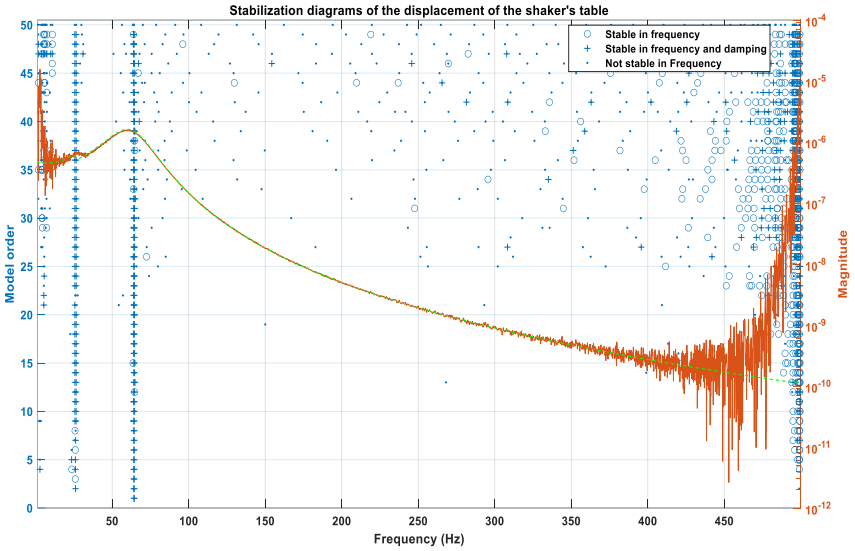

Figure 4. The stabilization diagrams comparison of the displacement of the shaker's table.

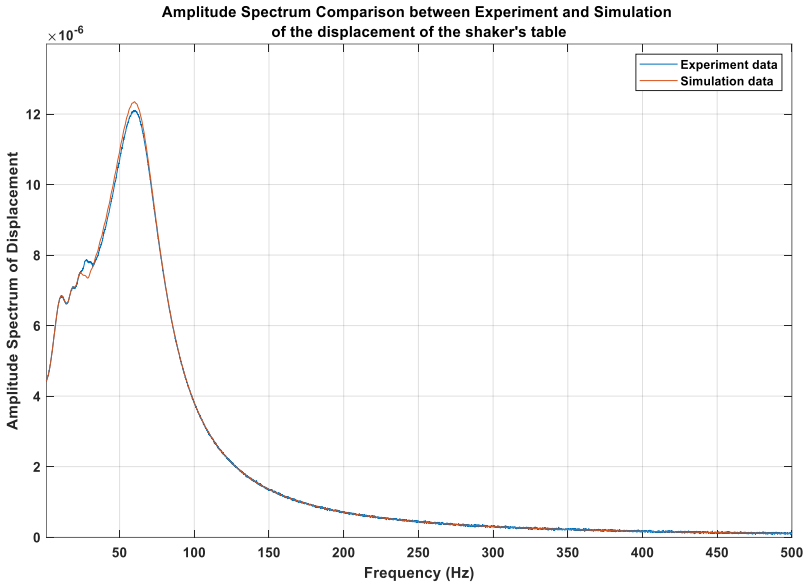

Figure 5. Comparison between experiment and simulation of the displacement amplitude spectrum of the shaker's table.

References

[1] GF. Lang. Electrodynamic Shaker Fundamentals[J], Sound and Vibration, **1997**, 31(4):14-23.
[2] GF. Lang, D. Snyder. Understanding the physics of Electrodynamic shaker performance[J], Sound and Vibration, **2001**, 35(10):24-33.
[3] M. Appolloni, A. Cozzani. Virtual Testing Simulation Tool for the New QUAD Head Expander Electrodynamic Shaker, Proceedings of the 6th International Symposium on Environmental Testing for Space Programmes, June 12-14 **2007**, ESTEC, Noordwijk.
[4] M. Remedia, G. Aglietti, M. Appolloni, et al. A virtual testing approach for spacecraft structures post-correlation purposes[R]. University of Surrey, **2016**.
[5] M. Remedia, G. Aglietti G, M. Appolloni, et al. Virtual testing: a pre-and post-test tool for base-driven spacecraft testing[C]//Aerospace Testing Seminar. **2017**.

[6] P. Nali, A. Bettacchioli, G. Landi, et al. A virtual shaker testing experience: Modeling, computational methodology and preliminary results. Advances in aircraft and spacecraft science, **2018**, 5(2): 251.
[7] A. Bettacchioli. Simulation of satellite vibration test[C]//13th European Conference on Spacecraft Structures, Materials & Environmental Testing. **2014**, 727: 51.
[8] S. Ricci, B. Peeters, J. Debille, et al. Virtual shaker testing: a novel approach for improving vibration test performance[C]//PROCEEDINGS OF ISMA 2008: INTERNATIONAL CONFERENCE ON NOISE AND VIBRATION ENGINEERING, VOLS. 1-8. KATHOLIEKE UNIV LEUVEN, DEPT WERKTUIGKUNDE, **2008**: 1767-1782.
[9] J. Martino, K. Harri. The shaker parameters estimation, a first step to virtual testing[C]//MATEC Web of Conferences. Edp Sciences, **2018**, 148: 05003.